Physics of Plasmas

Mechanism of non-steady Petschek-type reconnection with uniform resistivity

Cite as: Phys. Plasmas **26**, 032903 (2019); https://doi.org/10.1063/1.5084771
Submitted: 07 December 2018 . Accepted: 27 February 2019 . Published Online: 25 March 2019

Takuya Shibayama, Kanya Kusano, Takahiro Miyoshi, and Amitava Bhattacharjee

Physics of Plasmas ARTICLE scitation.org/journal/php

Mechanism of non-steady Petschek-type reconnection with uniform resistivity

Cite as: Phys. Plasmas **26**, 032903 (2019); doi: 10.1063/1.5084771
Submitted: 7 December 2018 · Accepted: 27 February 2019 ·
Published Online: 25 March 2019

Takuya Shibayama,[1,a)] Kanya Kusano,[1] Takahiro Miyoshi,[2] and Amitava Bhattacharjee[3,4,5]

AFFILIATIONS

[1]Institute for Space-Earth Environmental Research, Nagoya University, Furo-cho, Chikusa-ku, Nagoya, Aichi 464-8601, Japan
[2]Department of Physical Science, Graduate School of Science, Hiroshima University, Higashi-Hiroshima 739-8526, Japan
[3]Department of Astrophysical Sciences and Princeton Plasma Physics Laboratory, Princeton University, Princeton, New Jersey 08543, USA
[4]Max Planck/Princeton Center for Plasma Physics, Princeton University, Princeton, New Jersey 08543, USA
[5]Center for Computational Astrophysics, Flatiron Institute, New York, New York, 10010, USA

[a)]Electronic mail: shibayama@nagoya-u.jp

ABSTRACT

The Sweet-Parker and Petschek models are well-established magnetohydrodynamics (MHD) models of steady magnetic reconnection. Recent findings on magnetic reconnection in high-Lundquist-number plasmas indicate that Sweet-Parker-type reconnection in marginally stable thin current sheets connecting plasmoids can produce fast reconnection. By contrast, it has proven difficult to achieve Petschek-type reconnection in plasmas with uniform resistivity because sustaining it requires localization of the diffusion region. However, Shibayama *et al.* [Phys. Plasmas **22**, 100706 (2015)] recently noted that Petschek-type reconnection can be achieved spontaneously in a dynamical manner even under uniform resistivity through what they called *dynamical Petschek reconnection*. In this new type of reconnection, Petschek-type diffusion regions can be formed in connection with plasmoids. In this paper, we report the results of two-dimensional resistive MHD simulation with uniform resistivity, undertaken to determine the diffusion region localization mechanism under *dynamical Petschek reconnection*. Through this modeling, we found that the separation of the X-point from the flow stagnation point (S-point) plays a crucial role in the localization of the diffusion region because the motion of the X-point is restricted by the strong flow emanating from the flow stagnation point. This mechanism suggests that *dynamical Petschek reconnection* is possible even in large systems such as the solar corona.

I. INTRODUCTION

Magnetic reconnection is a fundamental process of energy conversion in astronomical, space, and laboratory plasmas.[2] Magnetic reconnection changes the connectivity of a magnetic field and converts magnetic energy into kinetic or thermal energy. Fast magnetic reconnection is necessary to explain the explosive energy release occurring during solar flares, magnetospheric substorms, and tokamak plasma disruptions. The key parameter of magnetic reconnection is the reconnection rate, M, which is a non-dimensional number given by normalizing the inflow velocity with the upstream Alfvén velocity ($M = V_{in}/V_A$). The reconnection rate during solar flares has been measured by detecting the inflow feature, or reconnected magnetic flux,[3,4] with the results suggesting that the average reconnection rate in the solar corona is of the order of 0.01. One of the goals of magnetic reconnection theory is to explain this reconnection rate.

In the 1950s and 1960s, several MHD theories describing steady state ($\partial/\partial t = 0$) magnetic reconnection were proposed. The Sweet-Parker model[5,6] predicts that the reconnection rate (M) is proportional to the inverse square root of the Lundquist number S ($= LV_A/\eta$, where L is the system size, V_A the Alfvén speed, and η the plasma resistivity), that is, $M \sim S^{-0.5}$. For large-S systems such as the solar corona ($S \sim 10^{12}$–10^{14}), the Sweet-Parker model predicts reconnection rates that are too small to account for observations. To solve this difficulty, Petschek proposed another reconnection model[7] in which efficient magnetic reconnection progresses over a small diffusion region and energy conversion occurs within slow-mode MHD shock layers. As the predicted reconnection rate is nearly independent of S, fast reconnection with $M = 0.01$ can be explained under this model. In systems with uniform resistivity, however, the Petschek model cannot maintain the small diffusion region.[8–10] It thus appears that the Petschek model is inapplicable to plasma with uniform resistivity.[11,12]

For the non-steady state case, magnetic reconnection with plasmoids is considered to be a fruitful model of MHD fast reconnection under uniform resistivity.[1,11–19] As sufficiently long current sheets are unstable to tearing instability,[15] the current sheets are divided into several secondary current sheets connecting closed magnetic field structures or plasmoids. The reduced length of these secondary current sheets corresponds to the reduced local Lundquist number, $S_{local} = L_{local} V_A/\eta$, and if there are a sufficient number of plasmoids, the intervening Sweet-Parker diffusion region can accommodate fast reconnection. For this reason, the new results on plasmoid-mediated magnetic reconnection can be understood heuristically as an extension of the Sweet-Parker argument.[11,12]

Another possible fast reconnection scenario under uniform resistivity is non-steady Petschek-type reconnection.[20] Recent advances in supercomputing power have enabled the direct numerical simulation of large-scale, high-S MHD magnetic reconnection regimes. As S increases beyond a threshold, the system produces more plasmoids and evolves dynamically. We previously noted that Petschek-type small diffusion regions spontaneously appear in the dynamic evolution of plasmoid reconnection even under uniform resistivity[1] and proposed the *dynamical Petschek reconnection* regime, in which small Petschek-type diffusion regions always appear in close contact with the ends of plasmoids and drive fast reconnection. This represents a potential new reconnection regime at high Lundquist numbers $S \gtrsim 10^6$. However, the detailed mechanism of the formation of Petschek-type diffusion regions is poorly understood, partly because the evolution of the system is highly dynamic, and to fully develop this theory, it will be necessary to uncover the mechanism of the formation of Petschek-type reconnection regions during nonlinear evolution.

Although it is not discussed in detail, similar current structures next to plasmoids are also observed in other simulation studies of high-Lundquist-number current sheets.[11,12,21] In particular, Fig. 3(f) in the study by Huang and Bhattacharjee[12] and the attached movie show the evolution of Petschek-like localized diffusion regions next to plasmoids. They report fast reconnection as a result of highly non-linear evolution of the current sheet, to which Petschek-type diffusion regions may contribute.

In this paper, we attempt to clarify the Petschek-type diffusion region formation mechanism by focusing on the non-linear resistive MHD simulation of a single Petschek-type diffusion region. To do this, we conducted a local numerical simulation of a diffusion region associated with a single plasmoid to model one of the Petschek-type diffusion regions within the global simulation carried out in the previous study.[1]

Section II introduces the initial and boundary conditions of the model. In Sec. III, we discuss the results of the formation mechanism of non-steady Petschek-type reconnection, while in Sec. IV, we discuss how the model can be applied to larger systems. Finally, we summarize our results in Sec. V.

II. MODEL

To better understand the fundamental formation process of the Petschek-type structure, we constructed a simple model employing time-dependent MHD simulation. The governing equations of the model are the following set of normalized compressible resistive MHD equations with uniform resistivity in the conservation form

$$\frac{\partial \rho}{\partial t} + \nabla \cdot (\rho \mathbf{V}) = 0, \tag{1}$$

$$\frac{\partial \rho \mathbf{V}}{\partial t} + \nabla \cdot \left[\rho \mathbf{V}\mathbf{V} + \left(p + \frac{B^2}{2}\right)\mathbf{I} - \mathbf{B}\mathbf{B}\right] = 0, \tag{2}$$

$$\frac{\partial \mathbf{B}}{\partial t} + \nabla \cdot (\mathbf{V}\mathbf{B} - \mathbf{B}\mathbf{V}) + \eta \nabla \times \mathbf{J} = 0, \tag{3}$$

$$\frac{\partial e}{\partial t} + \nabla \cdot \left[\left(e + p + \frac{B^2}{2}\right)\mathbf{V} - (\mathbf{V} \cdot \mathbf{B})\mathbf{B} + \eta \mathbf{J} \times \mathbf{B}\right] = 0, \tag{4}$$

where $e = p/(\gamma - 1) + \rho v^2/2 + B^2/2$ is the total energy density. The polytropic index is set to $\gamma = 5/3$. All other symbols have their standard meanings. We use standard Ohm's law in resistive MHD

$$\mathbf{E} = -\mathbf{V} \times \mathbf{B} + \eta \mathbf{J}. \tag{5}$$

Viscosity and thermal conduction are ignored. The numerical code is based on the Harten-Lax-van Leer Discontinuities (HLLD) scheme,[22] and the divergence-free property of the magnetic field is controlled by the Harten-Lax-van Leer flux Constrained Transport method.[23] The initial condition is the following Harris-type current sheet of width L_0 plus an initial perturbation:[24]

$$\mathbf{B}(x, y) = \mathbf{B}_0 \tanh(y/L_0) \tag{6}$$

$$p(x, y) = p_0 \left[\cosh^{-2}(y/L_0) + \beta\right], \tag{7}$$

where $\mathbf{B}_0 = (B_0, 0)$ and β denotes the upstream plasma beta, i.e., the ratio between the upstream gas and magnetic pressures. In our modeling, we used $\beta = 0.2$.

Since we construct this model to study the fundamental process of how a single diffusion region forms in the large-scale simulation,[1] we apply an initial condition and perturbation which are symmetric in both x and y directions to prevent the motion of the plasmoid. (As discussed later, the imposition of this symmetry has an effect on the reconnection rate but does not change qualitatively the physical mechanism, which is the focus of this paper.) We apply two initial perturbations to study the dependence on the initial condition. The initial perturbations of the magnetic field are given by the following vector potentials:

$$\mathbf{A}_1(x, y) = A_0 \left\{ \exp\left[-\left(\left(\frac{x - x_0}{\lambda_x}\right)^2 + \left(\frac{y}{\lambda_y}\right)^2\right)\right] + \exp\left[-\left(\left(\frac{x + x_0}{\lambda_x}\right)^2 + \left(\frac{y}{\lambda_y}\right)^2\right)\right]\right\} \hat{\mathbf{e}}_z, \tag{8}$$

or

$$\mathbf{A}_2(x, y) = -A_0 \left\{ \exp\left[-\left(\left(\frac{x}{\lambda_x}\right)^2 + \left(\frac{y}{\lambda_y}\right)^2\right)\right]\right\} \hat{\mathbf{e}}_z, \tag{9}$$

where $x_0 = 10L_0$, $\lambda_x = \lambda_y = 5L_0$, and $A_0 = 0.05$. Both the perturbations correspond to single isolated plasmoid with a double X-point at $\pm x_0$ or a single O-point at the origin.

The initial fluctuation perturbs the exact equilibrium. The final expansion phase discussed in Sec. III is, however, almost independent of the details of the initial condition.

The computational domain is $0 \le x \le L_x$, $0 \le y \le L_y$, where $L_x = 600L_0$ and $L_y = 50L_0$.

Here, L_x and L_y are set to be sufficiently large to minimize the effect of the boundary on the reconnection structure. As boundary conditions, reflection boundaries are set at $x=0$, $x = L_x$, and $y=0$, while the boundary at $y = L_y$ is a conducting wall. As the simulation proceeds, a plasmoid forms at the origin with its center (magnetic O point) fixed at the origin as a result of the boundary conditions, i.e., the symmetry of the system. This setup simplifies the analysis and evolutionary details of the diffusion region adjacent to the plasmoid. (Murphy[25] refers to the initial condition with $\mathbf{A}_1$ as a double perturbation.) The electric resistivity in the model is set at $\eta = 1/300$ to reproduce the local conditions in our previous large-scale simulation[1] (see Sec. IV for details). In the simulation, physical quantities are normalized to the following values: $B_0/\sqrt{4\pi}$, L_0, upstream plasma density $= \rho_0$, and upstream Alfvén velocity, $V_{A0} = B_0/\sqrt{4\pi\rho_0}$. Accordingly, other quantities are normalized as follows: $t_0 = L_0/V_{A0}$, $p_0 = B_0^2/(8\pi)$, $J_0 = B_0/(\sqrt{4\pi}L_0)$, and $F_0 = B_0^2/(4\pi L_0)$.

We use a non-uniform grid along the x and y directions that is almost uniform at $0 \le x \lesssim 200$, $0 \le y \lesssim 5$ and gradually expands in the $+x$ and $+y$ direction in order to minimize numerical diffusion and reduce the computational cost. The simulation setups are summarized in Table I. The largest grid number is 8192×2048, and the highest spatial resolution is $\Delta x = 3.5 \times 10^{-2}$ and $\Delta y = 5.1 \times 10^{-3}$ at around the origin (run 1). Most of the results in this paper are obtained from run 1. The results and discussion do not significantly change in the run with half of the grid number in both the directions (run 2) with the difference in the reconnection rate limited to less than 2%.

III. RESULTS

Figure 1 shows the distribution of out-of-plane current density J_z and outflow velocity V_x at $t=500$. A Petschek-type bifurcated current structure is observed at $15 \lesssim x \lesssim 125$ [Fig. 1(a)]. This current density structure is qualitatively similar to Petschek-type reconnection with anomalous resistivity[26] although the resistivity is uniform and the plasmoid is located at the origin in our simulation. The diffusion region is localized adjacent to the plasmoid, from which it can be inferred that the localization is related to the plasmoid and the surrounding plasma condition. The entire structure is similar to the one in Fig. 3 in the study by Shibayama *et al.*[1] Additionally, it is seen from Fig. 1(b) that the width of the reconnection outflow increases with the outflow toward the positive x direction: this structure is another important characteristic of Petschek reconnection.

In the latter phase ($t > 500$) after the formation of the Petschek-type diffusion region, the system shows gradual, self-similar-like expansion.

Note that in our simulation results, only the right-hand side of the Petschek model is formed, while the steady-state Petschek model is symmetric across the diffusion region.

TABLE I. Initial perturbations and grid settings.

	Initial perturbation	Grid number
Run 1	$\mathbf{A}_1$	8192×2048
Run 2	$\mathbf{A}_1$	4096×1024
Run 3	$\mathbf{A}_2$	4096×1024

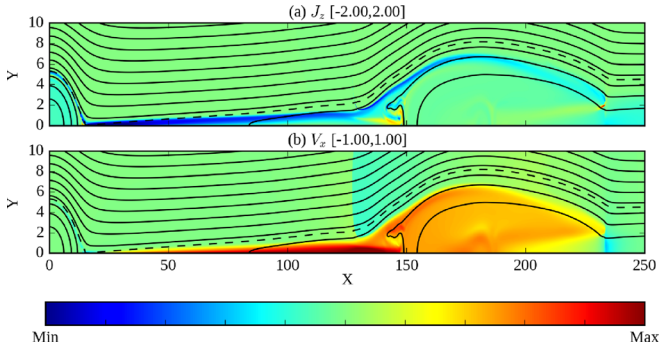

FIG. 1. Spatial distribution of out-of-plane current density J_z and outflow velocity V_x at $t=500$ for run 1. The color range is shown with the panel titles. Solid and dashed lines indicate the magnetic field lines and separatrix, respectively.

Figure 2 shows the detailed flow structure around the diffusion region. It is seen form Fig. 2(a) that the flow structure around the X-point is asymmetric, with the Petschek-type structure appearing only just to the right of the X-point, while the leftward outflow is very short and connected to the plasmoid. Figure 2(b) shows a line integral convolution plot of the flow structure, in which each pattern is aligned with the local velocity vector. It is seen that the inflow is primarily

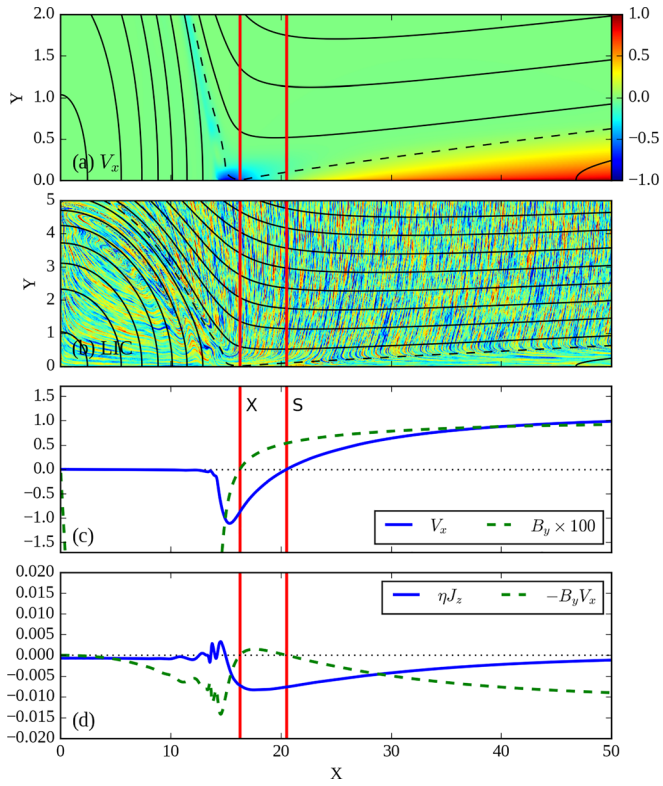

FIG. 2. (a) Outflow structure and (b) line integral convolution plot of the flow at $t=500$ for run 1. (c) Outflow and reconnected magnetic field profile and (d) terms in Ohm's law along $y=0$ at $t=500$ for run 1. All panels are aligned in the vertical direction. The vertical red solid lines in each panel show the location of the X- and S-points on the x-axis.

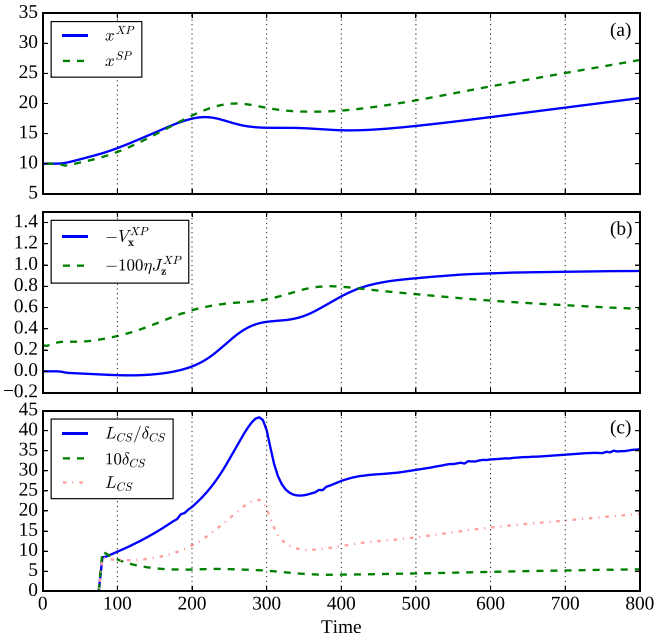

FIG. 3. (a) Location of the X- and S-points, (b) *x*-component of velocity at the X-point and the reconnection rate, and (c) length L_{CS}, thickness δ_{CS}, and aspect ratio of the diffusion region as functions of time for run 1.

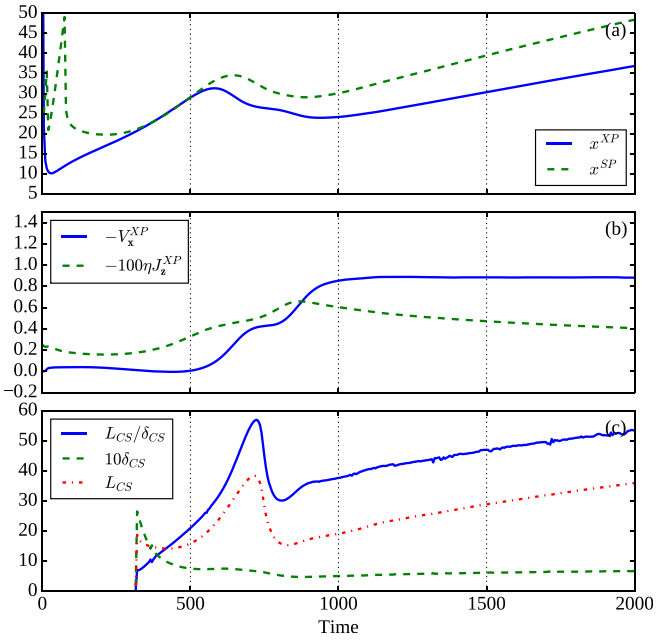

FIG. 4. The same as Fig. 3 but for run 3.

inclined to the left. Figure 2(c) shows a profile of the outflow velocity and reconnected magnetic field strength along $y = 0$. At $t = 500$, the X- and S-points are located at $x = 16.3$ and 20.5, respectively. The clear separation in the x direction results in a strong plasma flow at nearly the Alfvén velocity in the negative x direction at the X-point.

The localization of the diffusion region is seen from Fig. 2(d), which shows terms in the right hand side of Eq. (5) along $y = 0$. The resistive term is dominant in $15.5 < x < 28.9$, and the diffusion region is localized compared to the distance between the plasmoids, which is about 10 times larger than the diffusion region length.

The temporal evolution of physical quantities is shown in Fig. 3. Positions in the x direction of the X- and S-points (x^{XP} and x^{SP}, respectively) show that the S-point overtakes the X-point at $t \sim 200$ [Fig. 3(a)], which is also pointed out by Murphy.[25] The final expansion phase ($t > 500$) is, however, nearly independent of the initial behavior. Figure 4 shows the same plot for run 3, which shows qualitatively similar time evolution to that of run 1 except for the initial behavior of the X- and S-point location. Note that the range of the horizontal and vertical axes is different between Figs. 3 and 4. Figure 3(b) shows the plasma velocity at the X-point V_x^{XP} and the reconnection rate as a function of time. The reconnection rate is defined as ηJ_z at the X-point, which corresponds to the reconnection rate normalized by the initial upstream quantities. V_x^{XP} increases to ~ 0.4 at $t = 300$ and reaches almost 1 in the final expansion phase($t > 500$). The reconnection rate increases up to about 0.008 and decreases as the structure expands. This reconnection rate is smaller than our previous results.[1] The difference may be explained by the asymmetry in the x-direction (see Sec. IV for detail). Figure 3(c) shows the geometry of the current sheet. The current sheet is defined as the region, where the $\eta \boldsymbol{J}$ term is dominant in Eq. (5) ($\eta|\mathbf{J}| > |\mathbf{V} \times \mathbf{B}|$). The length L_{CS} and the thickness δ_{CS} of the current sheet are measured from the X-point to the x and y directions, respectively. Since the current sheet is asymmetric in the x direction, L_{CS} and δ_{CS} are the full length and thickness of the current sheet. We do not define L_{CS} and δ_{CS} in the initial phase ($t < 80$) because the current sheet is not formed yet. The aspect ratio of the current sheet L_{CS}/δ_{CS} increases and peaks at $t \sim 300$ and then decreases when $V_x^{XP} \simeq -0.4$.

If symmetry is assumed to be around the neutral line ($y = 0$), the x-component of the equation of motion and the y-component of the induction equation on the neutral line can be written as follows:

$$\rho d_t V_x = F_x^{PR} + F_x^L, \tag{10}$$

$$\partial_t B_y = -\partial_x (V_x B_y) + \eta \partial_x J_z, \tag{11}$$

where ∂_x and d_t represent the differential operators $\partial/\partial x$ and d/dt, respectively, and F_x^{PR} and F_x^L are the pressure gradient force $F_x^{PR} = -\partial_x P$ and Lorentz force $F_x^L = -J_z B_y$, respectively. Figure 5 plots each term in Eqs. (10) and (11) against x. In Fig. 5(a), it is seen that the rightward outflow plasma is accelerated by the Lorentz force F^L, a characteristic of the Petschek model. By contrast, outward flow to the left is accelerated by the gas pressure gradient force F^{PR}, a characteristic of the Sweet-Parker model.

It is seen from Fig. 5(b) that the terms on the right-hand side of Eq. (11) nearly cancel to the right of the X-point. As a result, the variation of B_y over time is minimal, and the system is in a quasi-steady state. The evolution of the system actually shows a self-similar-type gradual expansion. These results suggest that the state is a close to self-similar solution of the MHD equations: Nitta[27] noted the existence of such a solution with a plasmoid at the origin.

IV. DISCUSSION

In Sec. III, we presented simulation results indicating Petschek-type reconnection in a system with uniform resistivity, in which the

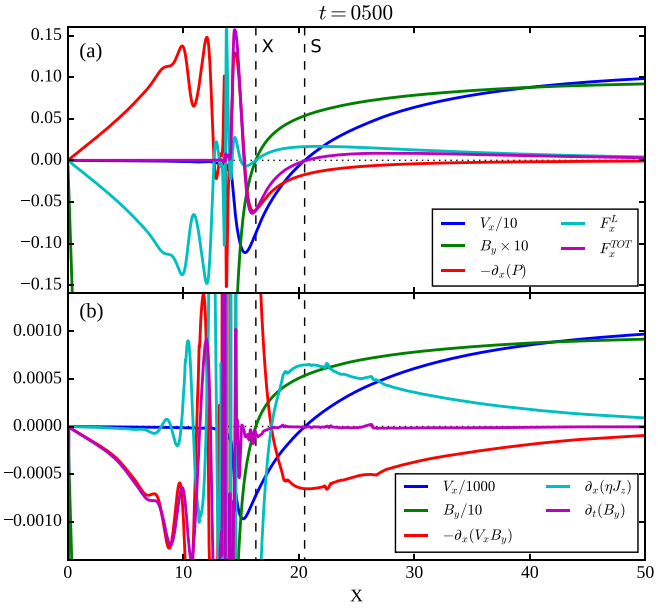

FIG. 5. Each term of (a) the *x*-components of the equation of motion and (b) the *y*-components of the induction equation along the neutral plane $y = 0$ at $t = 500$ for run 1. The vertical dashed lines show the locations of the X- and S-points. Here, we note that there is a large fluctuation at $10 < x < 15$ as a result of the termination shock of the leftward outflow.

separation of the X-point from the flow stagnation point is observed. In this section, we discuss the evolution of the location of the X- and S- points and how this works as a localization mechanism in the *dynamical Petschek reconnection* regime.[1]

According to Murphy,[25] the velocity of apparent motion of the X-point V_{XP} is determined using the following equation:

$$V_{XP} \simeq \left(V_x - \frac{\eta}{\partial_x B_y} \partial_y^2 B_y \right)_{X-point}. \quad (12)$$

The first term on the right-hand side of this equation corresponds to the ideal MHD contribution, while the other term is the resistive factor. In our simulation, plasma flow occurs at the X-point as a result of the separation of the X- and S-points. This flow, which corresponds to the first ideal term in Eq. (12), prevents the motion of the X-point. As the X-point is located near the plasmoid, this results in localization of the diffusion region. By contrast, in the classical symmetric reconnection case, the X- and S-points coincide, and therefore, the plasma velocity is zero at the X-point. The separation of the X- and S-points is the key characteristic of Petschek-type reconnection under uniform resistivity.

In addition to the local flow structure discussed above, the global eddy structure in the inflow region plays an important role in the plasma dynamics. As the plasmoid instability evolves, large eddies form in the inflow region.[28] It is seen from Fig. 2(b) that the diffusion region is embedded in the eddy around the plasmoid: accordingly, the inflow velocity has a negative *x* component prior to entering the diffusion region. The eddy evolves as the plasmoid grows non-linearly, modifying both the velocity and the magnetic field structures in the inflow region.

In our model, we use a spatially and temporally constant electric resistivity $\eta = 1/300$ for the current sheet with the thickness of $L_0 = 1$. This setting corresponds to the sheet occurring in our previous simulation[1] following re-normalization. In the $S_0 = 10^4$ run ($\eta = 10^{-4}$), the typical current sheet thickness prior to the formation of the plasmoid and Petschek-type structure was 1/20–1/30.

It is well known that a resistive MHD system is characterized by a single non-dimensional number—magnetic Reynolds number $R_m = lv/\eta$. Using the initial current sheet thickness and upstream Alfvén speed as typical values, in our model, $R_m = 300$.

This specific value of the magnetic Reynolds number is related to Eq. (12), in which, the first ideal term has a value of the order of one owing to the outflow. By contrast, it is seen from Fig. 2(a) that the speed of the X-point propagation is of the order of 0.01. The following resistive term in the formula must almost compensate for the ideal term when the system is in the slow expansion phase. The term contains η and the spatial gradient of the magnetic field. When η is small, the Lundquist number is large, and the length scale of the structure should be proportionally small, resulting in R_m on the same order of magnitude, which is 300 in our results.

Although the Lundquist number, *S*, is also a non-dimensional parameter, the global system size is used as the typical length. Even in high Lundquist number systems, the local magnetic Reynolds number can become as small as 300 when the current sheet is sufficiently thin, allowing the Petschek-type structure reported in this paper to appear. This mechanism determines the reconnection rate in *dynamical Petschek reconnection*, in which the rate is driven by the Petschek-type structure.

In the model described in this paper, asymmetry between diffusion regions grows as a result of the initial and boundary conditions. In general, this asymmetry can be initiated and sustained for several reasons, e.g., initial or boundary conditions, unidirectional flow, or plasmoid motion. A similar process also occurs in plasmoid reconnection at high Lundquist numbers.[1] Figure 6 shows the outward flow velocity and current density before and after the formation of plasmoids under the simulation at $S_0 = 10^4$ in the study by Shibayama *et al.*[1] A chain of three plasmoids is visible, with Petschek-type structures forming on both sides of the plasmoid chain at around $x = 280$ and 320, although not on both sides of all plasmoids. In this case, the plasma flow serves as the origin of asymmetry. Prior to the formation of the plasmoids [Fig. 6(a)], a Sweet-Parker reconnection region is present. Although the outward flow structure is globally symmetric, when the plasmoids form within the system, the flow in the current sheet is

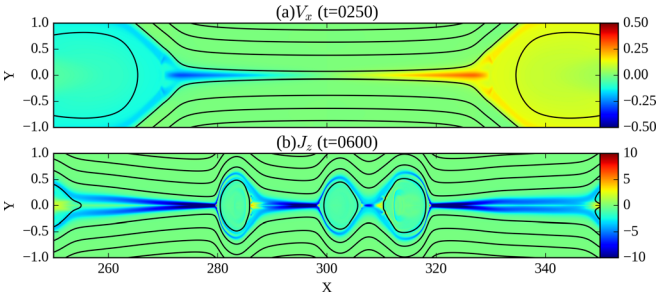

FIG. 6. (a) Initial Sweet-Parker outflow from a high-Lundquist number simulation.[1] (b) Plasmoids and Petschek-type current structure formed in the outflow.

directed to either the left or the right. In this case, the downstream side of the plasmoids is preferable for the formation of Petschek-type diffusion regions [Fig. 6(b)].

In the frame of reference of the plasmoid, the ambient plasma flows against the plasmoid in the downstream side. This opposing flow strengthens the ideal term of Eq. (12) and facilitates the localization of the diffusion region. The plasma velocity at the X-point in this study is about V_A (see Fig. 2), while the speed of plasmoid motion is, in general, also Alfvénic. The opposing flow also affects the reconnection rate, which is 0.008 in this paper and 0.02 in our previous results. This effect, which is caused by the asymmetry in the x-direction, is very likely the reason underlying the difference in the reconnection rates in the two simulations. By contrast in the upstream side, the ambient flow weakens the localization of the diffusion region.

From Fig. 6(b), it is also seen that the curvature radius of the magnetic field at around $x = 280$ is smaller on the left-hand side of the nearby plasmoid because the leftward motion of the plasmoid leads to a steepening of the left-hand face of the plasmoid. These are plausible explanations for the appearance of a Petschek-type structure at only the left-hand side of the plasmoid. The three plasmoids and the neighboring Petschek-type diffusion region drive fast reconnection until the plasmoids eventually collide, terminating the reconnection until the next set of plasmoids and the Petschek-type diffusion region appear. The quasi-periodic modulation of the reconnection rate is generated by the sequence of formation and coalescence of plasmoids.

We next compare our results with those of a previous model of Petschek-type reconnection with uniform resistivity by Kulsrud,[9] in which the Petschek-type diffusion region cannot retain its structure in the steady state because the uniformly resistive system does not have a mechanism to localize the diffusion region. In our model, by contrast, the diffusion region is localized and Petschek-type reconnection is achieved even under uniform resistivity. There are a few differences between our results and the theory in the study by Kulsrud.[9] The most important difference is in the profile of magnetic field strength in the inflow region. Kulsrud[9] assumes an upstream profile $B_x = B_0(1 - x^2/L^2)$, where L denotes the global system size. This means that B_x gradually decays with the system size.

The profile of B_x in the inflow region is shown in Fig. 7. The dashed line is a parabolic curve of $B_x = 1 - (x - 20)^2/130^2$, which leads to Sweet-Parker reconnection according to Kulsrud.[9] In our numerical simulation, the upstream profile of B_x decays more steeply especially around the center of the diffusion region $20 \lesssim x \lesssim 50$.

The steep profile of B_x is formed in a self-consistent manner as a result of the evolution of the plasmoid and surrounding plasma flow, indicating that a Petschek-type diffusion region can spontaneously form in a non-steady system even under uniform resistivity.

Baty, Forbes, and Priest[29] also discuss the stability of Petschek reconnection under spatially localized resistivity and report that asymmetric Petschek reconnection is stable in resistivity profiles that are flatter than Gaussian. Our results show that asymmetric Petschek reconnection is stable under uniform resistivity, which is a flat limit of the resistivity profile. Accordingly, our results are qualitatively consistent with the result in the study by Baty, Forbes, and Priest.[29]

Priest and Forbes[30] proposed a generalized model of fast steady state magnetic reconnection including the Petschek model and the Sonnerup model[31] as special cases. Figure 8 shows gas pressure, magnetic pressure, and V_x along $x = 100$. It is seen that the profiles of gas and magnetic pressure show the same behavior as the Petschek model, which shows almost constant pressure in the inflow region (see Fig. 9 in the study by Yan *et al.*[32]).

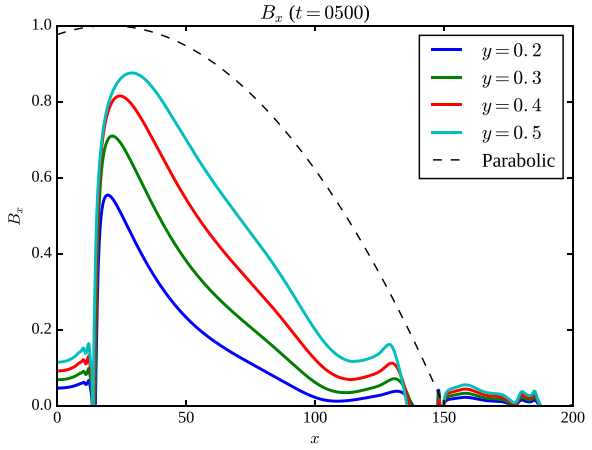

FIG. 7. Profile of the reconnecting magnetic field B_x in the inflow region at different y values at $t = 500$ for run 1, as well as a parabolic curve, which is the assumption in the study by Kulsrud.[9]

V. CONCLUSION

In the context of the nonlinear plasmoid theory, our model results demonstrate Petschek-type reconnection even with a spatially uniform resistivity. Using boundary conditions to fix the plasmoid, we successfully model the fundamental formation process of the Petschek-type structure which appears in our previous large-scale simulation.[1] In our results, the X-point is adjacent to a plasmoid, which blocks any extension of the diffusion region because the X- and flow stagnation points are separated by the presence of the plasmoid. As a result, a strong plasma flow is present at the X-point, the diffusion region is localized, and a Petschek-type reconnection region forms even under uniform resistivity. Prior to the formation of the Petschek-type structure, the local magnetic Reynolds number, R_m, of the current sheet is approximately 300.

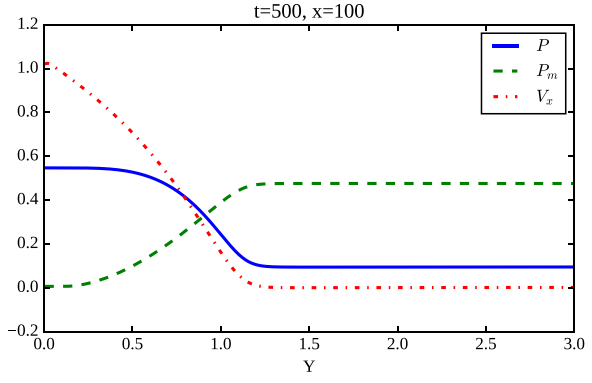

FIG. 8. Profile of the gas pressure, magnetic pressure, and V_x at $x = 100$ along the y direction for run 1.

The process of fast reconnection realized by the plasmoid instability is a dynamic phenomenon, in which a system-size thin current sheet breaks up into plasmoids connected by thin current sheets. Huang and Bhattacharjee[12] have suggested that the process can be understood on the basis of a heuristic model in which thin current sheets are essentially thought of as short Sweet-Parker layers that are marginally stable. While this picture gives a good account of the reconnection rate (∼0.01) in the resistive MHD model, it is also seen in simulations that some of the fragmented current sheets do not have the time to stretch out to form Sweet-Parker layers but can be more aptly thought of as dynamical Petschek-type layers of the kind discussed in this paper. Both pictures appear to be consistent with the fast reconnection rate seen in plasmoid-mediated reconnection.

ACKNOWLEDGMENTS

This work was supported by JSPS/MEXT KAKENHI Grant Nos. 16J06873, JP15H05814, and JP15K04756. This research was supported by MEXT as "Exploratory Challenge on Post-K computer" (Elucidation of the Birth of Exoplanets [Second Earth] and the Environmental Variations of Planets in the Solar System). The results are obtained by using the K computer at the RIKEN Advanced Institute for Computational Science (Proposal number hp170077). A part of the computation was performed on the FX100 supercomputer system at the Information Technology Center, Nagoya University, and also on the Earth Simulator with the support of JAMSTEC. This study was carried out by using the computational resource of the Center for Integrated Data Science, Institute for Space-Earth Environmental Research, Nagoya University through the joint research program. A.B. acknowledges the support of NSF Grant Nos. AGS-1338944 and AGS-0962698 and the generous hospitality of the Center of Computational Astrophysics at the Flatiron Institute. Finally, we sincerely thank the anonymous referees for useful suggestions that helped improve the content of this paper.

REFERENCES

[1]T. Shibayama, K. Kusano, T. Miyoshi, T. Nakabou, and G. Vekstein, "Fast magnetic reconnection supported by sporadic small-scale Petschek-type shocks," Phys. Plasmas **22**, 100706 (2015).
[2]M. Yamada, R. Kulsrud, and H. Ji, "Magnetic reconnection," Rev. Mod. Phys. **82**, 603–664 (2010).
[3]T. Yokoyama, K. Akita, T. Morimoto, K. Inoue, and J. Newmark, "Clear evidence of reconnection inflow of a solar flare," Astrophys. J. **546**, L69–L72 (2001).
[4]H. Isobe, H. Takasaki, and K. Shibata, "Measurement of the energy release rate and the reconnection rate in solar flares," Astrophys. J. **632**, 1184–1195 (2005); e-print arXiv:astro-ph/0507327.
[5]P. A. Sweet, "The neutral point theory of solar flares," in *Electromagnetic Phenomena in Cosmical Physics*, IAU Symposium Vol. 6, edited by B. Lehnert (Cambridge University Press, 1958), p. 123, see http://ads.nao.ac.jp/abs/1958IAUS....6..123S.
[6]E. N. Parker, "Sweet's mechanism for merging magnetic fields in conducting fluids," J. Geophys. Res. **62**, 509–520, https://doi.org/10.1029/JZ062i004p00509 (1957).
[7]H. B. Petschek, "Magnetic field annihilation," NASA Spec. Publ. **50**, 425 (1964), see http://ads.nao.ac.jp/abs/1964NASSP..50..425P.
[8]D. Biskamp, "Magnetic reconnection via current sheets," Phys. Fluids **29**, 1520–1531 (1986).
[9]R. M. Kulsrud, "Magnetic reconnection: Sweet-Parker versus Petschek," Earth, Planets, Space **53**, 417–422 (2001); e-print arXiv:astro-ph/0007075.
[10]R. M. Kulsrud, "Intuitive approach to magnetic reconnection," Phys. Plasmas **18**, 111201 (2011).
[11]A. Bhattacharjee, Y.-M. Huang, H. Yang, and B. Rogers, "Fast reconnection in high-Lundquist-number plasmas due to the plasmoid instability," Phys. Plasmas **16**, 112102 (2009); e-print arXiv:0906.5599 [physics.plasm-ph].
[12]Y.-M. Huang and A. Bhattacharjee, "Scaling laws of resistive magnetohydrodynamic reconnection in the high-Lundquist-number, plasmoid-unstable regime," Phys. Plasmas **17**, 062104 (2010); e-print arXiv:1003.5951 [physics.-plasm-ph].
[13]H. P. Furth, J. Killeen, and M. N. Rosenbluth, "Finite-resistivity instabilities of a sheet Pinch," Phys. Fluids **6**, 459–484 (1963).
[14]*Plasma Astrophysics*, Frontiers in Physics Vol. 98, edited by T. Tajima and K. Shibata (Addison-Wesley, Reading, MA, 1997), p. QB462.7.T35.
[15]N. F. Loureiro, A. A. Schekochihin, and S. C. Cowley, "Instability of current sheets and formation of plasmoid chains," Phys. Plasmas **14**, 100703 (2007); e-print arXiv:astro-ph/0703631.
[16]K. Shibata and S. Tanuma, "Plasmoid-induced-reconnection and fractal reconnection," Earth, Planets, Space **53**, 473–482 (2001); e-print arXiv:astro-ph/0101008.
[17]N. F. Loureiro, R. Samtaney, A. A. Schekochihin, and D. A. Uzdensky, "Magnetic reconnection and stochastic plasmoid chains in high-Lundquist-number plasmas," Phys. Plasmas **19**, 042303 (2012); e-print arXiv:1108.4040 [astro-ph.SR].
[18]Y.-M. Huang, L. Comisso, and A. Bhattacharjee, "Plasmoid instability in evolving current sheets and onset of fast reconnection," Astrophys. J. **849**, 75 (2017); e-print arXiv:1707.01863 [physics.plasm-ph].
[19]L. Comisso, M. Lingam, Y.-M. Huang, and A. Bhattacharjee, "Plasmoid Instability in Forming Current Sheets," Astrophys. J. **850**, 142 (2017); e-print arXiv:1707.01862 [astro-ph.HE].
[20]H. Baty, "On the onset of the plasmoid instability," Phys. Plasmas **19**, 092110 (2012).
[21]Y.-M. Huang, A. Bhattacharjee, and T. G. Forbes, "Magnetic reconnection mediated by hyper-resistive plasmoid instability," Phys. Plasmas **20**, 082131 (2013); e-print arXiv:1308.1871 [physics.plasm-ph].
[22]T. Miyoshi and K. Kusano, "A multi-state HLL approximate Riemann solver for ideal magnetohydrodynamics," J. Comput. Phys. **208**, 315–344 (2005).
[23]T. Miyoshi and K. Kusano, "A comparative study of divergence-cleaning techniques for multi-dimensional MHD schemes," Plasma Fusion Res. **6**, 2401124 (2011).
[24]E. G. Harris, "On a plasma sheath separating regions of oppositely directed magnetic field," Il Nuovo Cimento **23**, 115–121 (1962).
[25]N. A. Murphy, "Resistive magnetohydrodynamic simulations of X-line retreat during magnetic reconnection," Phys. Plasmas **17**, 112310 (2010); e-print arXiv:1009.1875 [astro-ph.SR].
[26]S. Zenitani and T. Miyoshi, "Magnetohydrodynamic structure of a plasmoid in fast reconnection in low-beta plasmas," Phys. Plasmas **18**, 022105 (2011); e-print arXiv:1101.2255 [physics.space-ph].
[27]S.-Y. Nitta, "Continuous transition from fast magnetic reconnection to slow reconnection and change of the reconnection system structure," Astrophys. J. **663**, 610–624 (2007); e-print arXiv:astro-ph/0703008.
[28]G. Lapenta, "Self-feeding turbulent magnetic reconnection on macroscopic scales," Phys. Rev. Lett. **100**, 235001 (2008); e-print arXiv:0805.0426 [physics.plasm-ph].
[29]H. Baty, T. G. Forbes, and E. R. Priest, "The formation and stability of Petschek reconnection," Phys. Plasmas **21**, 112111 (2014).
[30]E. R. Priest and T. G. Forbes, "New models for fast steady state magnetic reconnection," J. Geophys. Res. **91**, 5579–5588, https://doi.org/10.1029/JA091iA05p05579 (1986).
[31]B. U. Ö. Sonnerup, "Magnetic-field re-connexion in a highly conducting incompressible fluid," J. Plasma Phys. **4**, 161–174 (1970).
[32]M. Yan, L. C. Lee, and E. R. Priest, "Fast magnetic reconnection with small shock angles," J. Geophys. Res. **97**, 8277–8293, https://doi.org/10.1029/92JA00170 (1992).